Classification of light charged particles via learning-based system identification

Mirko Mazzoleni, Matteo Scandella, Simone Formentin and Fabio Previdi

***Abstract*— This paper presents a nonparametric learning approach for the automatic classification of particles produced by the collision of a heavy ion beam on a target, by focusing on the identification of isotopes of the most energic light charged particles (LCP). In particular, it is shown that the measurement of the particle collision can be traced back to the impulse response of a linear dynamical system and, by employing recent kernel-based approaches, a nonparametric model is found that effectively trades off bias and variance of the model estimate. Then, the smoothened signals can be employed to classify the different types of particles. Experimental results show that the proposed method outperforms the state of the art approaches. All the experiments are carried out with the large detector array CHIMERA (Charge Heavy Ions Mass and Energy Resolving Array) in Catania, Italy.**

I. Introduction

One of the most interesting goals of the intermediate energy heavy ion research is to investigate the characteristics of the nuclei under extreme conditions of density and temperature [1]. In these types of physics' experiments, the standard approach is the measurement and analysis of the collision effects of a heavy ion beam over a target. The nuclear reactions induced by the nucleus-nucleus collision produce a large number of fragments with different energy, charge and mass values. This multifragmentation is predicted to be the major decay mode produced for a nuclear system at high density and temperature [5]. Thus, a complete experimental investigation, that should identify almost all the produced fragments, needs to ground on a suitable experimental device able to capture the particles that move away from the collision point in all directions. These devices present specific detector cells that generate an electrical signal when hit by a particle. The availability of these detectors, however, does not automate the classification of the detected particles' fragments. Infact, this task is often performed manually by visual inspection of the measured electrical quantities. An efficient automatic algorithm is therefore strongly advised.

One of the first attempts to develop a fully automated algorithm for isotopic classification of the most energetic light charged particles (LCP) has been presented in [12]. Here, the authors tackled the problem from a system identification point of view, identifying the dynamical system that generated the measurements. In this paper, we extend previous research by employing *kernel methods* for system identification, following the advice given in [7] (based on the separation/invariance principle) to *always first model as well as possible*. A model reduction step is then performed by means of a numerical algorithm for subspace state space system identification (N4SID) method [8].

Kernel methods are *nonparametric* learning techniques that very recently undergone a large interest from the system identification community [9], [10], [11]. They are based on the definition of a *kernel function* $k : \Omega \times \Omega \to \mathbb{R}$, with Ω a generic set where the input regressors belong, that embodies the properties of the functional space in which the desired function has to be searched. The main advantage is that they are shown to effectively trade off the bias/variance of the identification procedure, outperforming classical Prediction Error Methods (PEM) equipped with model selection criteria such as Akaike Information Criterion (AIC) [11]. The separation principle perfectly apply with these approaches. First, given data and prior information on the system behaviour, fit a low-bias and minimum variance model. Then, perform a further approximation via model reduction. The prior information is used to design the kernel function employed.

In light of the previous sections, the innovative contributions of this paper are three-fold: i) we propose the framework of Gaussian Processes (GP) [2] to first fit a low-bias model, followed by a N4SID model reduction step, in order to model the nuclear measurements; ii) we employ for the first time (as far as the authors are aware) the *stable spline kernel* [11] within a real world experimental setting; iii) we propose a black-box classification scheme that is taylored to the application and that highlights interpretability of its predictions.

II. Problem statement and experimental setup

The detector considered in this work is the large detector array CHIMERA (Charge Heavy Ions Mass and Energy Resolving Array) [1], installed at Laboratori Nazionali del Sud (Catania, Italy), see Figure 1.

The CHIMERA detector is designed for the study of heavy ion reactions at intermediate energy (up to 100MeV/nucleon). The multifragmentation phenomenum (i.e. the focus of this work) is produced by a beam of accelerated nuclei delivered by a superconducting cyclotron over a thin target, placed inside a vacuum chamber. When an accelerated nucleus collides over a target one, the hot and compressed system formed in the early stage of the collision can de-excite, leading to the generation of many fragments

M. Mazzoleni, M. Scandella and F. Previdi are with the Department of Management, Information and Production Engineering, University of Bergamo, Via G. Marconi 5, 24044 Dalmine (BG), Italy. S. Formentin is with the Department of Electronics, Information and Bioengineering, Politecnico di Milano, via G. Ponzio 34/5, 20133 Milano, Italy. Email to: mirko.mazzoleni@unibg.it.

Fig. 1: The CHIMERA detector array

with different charge, mass and energy. CHIMERA perceives the sorrounding phenomena by means of detection cells. Each detection cell is a telescope composed of a CsI(Tl) scintillation crystal with a thin Si detector in front of it. When it by a particle, the CsI(Tl) element produces a light impulse. A photodiode collects the emitted light producing a current output which is converted into a measurable voltage signal $v(t)$ via a charge amplifier. Similarly, the output of the Si detector (produced by a charge displacement when hit by a particle) is fed into a preamplifier and a signal $u(t)$ is generated. The measurement chain is depicted in Figure 2.

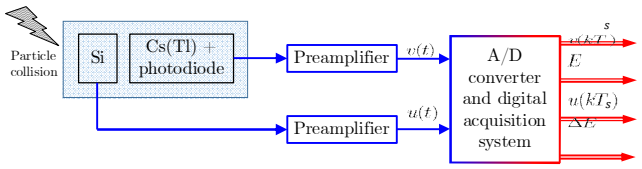

Fig. 2: Measurement chain, representing analog signals (blue) and digital signals (red)

The signal $v(t)$ is the most informative for the classification of LCP particles [12], [14]. The produced impulse measurements can be modeled by an exponetial law which decay rate depends on two time constants, a "fast" one (τ_f), and a "slow" one (τ_s) [15]. The voltage signal $v(t)$ is sampled at $T_s = 10$ns with a 14-bit resolution. For each pulse, 2048 samples are measured. A set of pulses produced by known particles (manually labeled with visual methods [12]) are collected in an experiment where a beam of 20Ne at 21MeV per nucleon bombards a ^{12}C target. The dataset employed for this work consists of 8751 pulses, about 20μs long, described in Table I. A total of 10 different particle types are considered. Particles with atomic number $Z \geq 5$ and with atomic mass number $A \geq 10$ are regarded as Heavy Ions.

The next section describes the following aspect: a) the observation motivating the modeling of the CsI(Tl) light impulse as the impulse response of a LTI system; b) the preprocessing steps performed on the raw measured data; c) the nonparametric smoothing procedure performed by means of gaussian processes; d) the subspace system identification technique employed using the smothened data.

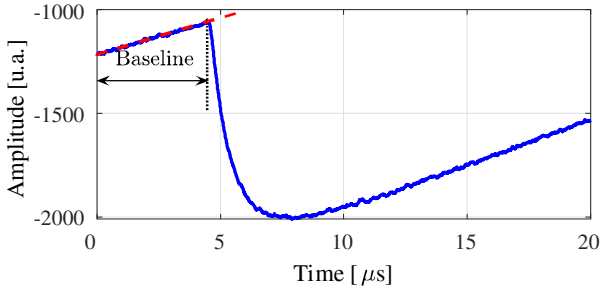

Fig. 3: Example of a measured $v(t)$ response (blue). The baseline value is highlighted with its fitted line (dotted red)

III. Modeling the Impulse Response

A. Working assumptions

Following the results in [12], we chose to model the signal $v(t)$, measured from the CsI(Tl) detector, as the impulse response of a Single-Input Single-Output (SISO) LTI system, with transfer function $V(s)$. Based on [12] and references therein, the following dynamic system model is employed:

$$V(s) = \frac{1}{1+s\tau_m} \cdot \left(\frac{\mu_f}{1+s\tau_f} + \frac{\mu_s}{1+s\tau_s} \right), \qquad (1)$$

where τ_f and τ_s denotes the fast and slow time constant of the light impulse response, respectively, the gains μ_f and μ_s are related to the energy of the particle, and τ_m models the dynamic respose of a unitary-gain sensor. Notice how, in this case, the time constant of the sensor is higher than the phenomenum that it is measured. Furthermore, we suppose that the data are affected by a stationary zero-mean additive noise, such that:

$$\widetilde{v}(kT_s) = v(kT_s) + e(kT_s), \quad k = 1, \ldots, 2048 \qquad (2)$$

where $\widetilde{v}(kT_s)$ denotes the noisy impulse response. From now on, we simplify the notation by dropping the term T_s in (2).

B. Preprocessing steps

A set of preprocessing steps have been performed on raw data. An example of measured impulse response is shown in Figure 3. It is possible to observe a "deadzone" prior to the impulse's starting. This is due to the post-triggering acquisition setup and acquisition chain's offsets. Thus, two actions are mandatory: i) the baseline removal and ii) the detection of the impulse starting time. The baseline removal process is made by fit a line on the first 4μs of the measurement, such that $g(k) = m \cdot k + l$, with $m, l \in \mathbb{R}$ the line's coefficients. The fitted line is then removed from the measurements, obtaining the signal $z(k) = \widetilde{v}(k) - g(k)$.

The detection of the starting time required special treatment, since impulses have different amplitudes and shapes. The following procedure was devised by the authors:

1) The discrete time derivative of $z(k)$ is computed $dz(k) = \big(z(k) - z(k-1)\big)/T_s$. A first estimate, i.e. k_1,

TABLE I: Dataset employed in this work

Isotope	Atomic number (Z)	Atomic mass number (A)	Number of employed pulses
^{1}H (protons)	1	1	904
^{2}H (deuterons)	1	2	980
^{3}H (tritons)	1	3	992
^{3}He	2	3	989
^{4}He	2	4	991
^{6}Li	3	6	989
^{7}Li	3	7	897
^{7}Be	4	7	510
^{9}Be	4	9	524
Heavy ions	≥ 5	≥ 10	979

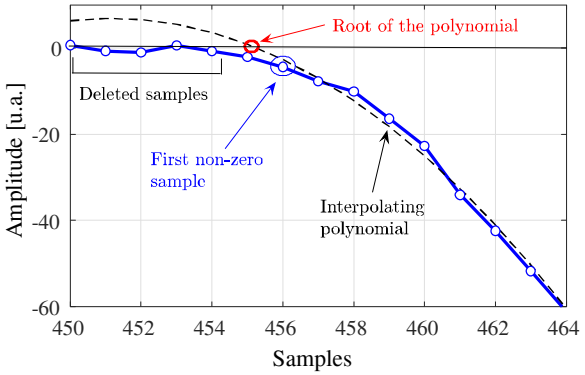

Fig. 4: The rationale for choosing the starting time

of the initial condition is made when $dz(k)$ exceedes a predefined threshold;

2) A third order polynomial $p(t)$ is fit on the 10 points after k_1;
3) The root r of $p(t)$ that is nearest to k_1 is computed. The nearest sampled point k_3 successive to r is taken as the first non-null impulse sample;
4) The starting point k^* is taken as the time instant before k_3, posing $z(k^*) = 0$. Samples before k^* are deleted. We denote the final preprocessed signal as $y(k), k = 1, \ldots, N$, where N is the length of the particular measurement (since the baseline length is different for each acquisition, the cleaned data can have different lengths).

The procedure is depicted in Figure 4 after that the baseline was removed. Each impulse now lasts about 16μs. The last caution was to multiply the data for minus one, in order to obtain an impulse response of a system with positive gain, as should be from physics relations.

C. Nonparametric system identification

Adhering to the rationale presented in the introduction, we chose to use the framework of gaussian processes to model the time-domain impulse responses. In this way, a low-bias and flexible model is obtained. The estimated response is the minimun variance estimate when error measurements and data are considered as Gaussian random variables. Given that the data are interpreted as impulse responses, the use of the *stable spline kernel* is the most natural choice. This is a particular type of kernel function that has been designed in order to model LTI systems. We employed the so called continous-time *second-order stable spline kernel* [11]:

$$k(s,t) = \lambda \cdot \left(\frac{e^{-\beta \cdot (s+t+\max(s,t))}}{2} - \frac{e^{-3\beta \cdot \max(s,t)}}{6} \right), \quad (3)$$

where $s, t \in \Omega \subset \mathbb{R}^+$ are generic continous-time instants, and $\lambda, \beta \in \mathbb{R}^+$ are hyperparameters that determine the shape of the kernel function (and therefore of the estimated one). Since, in this scenario, the function that we want to estimate is an impulse response, the domain of the kernel is the continuous time. Thus, the regressors are the time instants of the measurements.

Consider now the vector $Y \in \mathbb{R}^{N\times 1}$ formed by stacking the impulse response's values $y(k)$. As stated in (2), we can model the measurements as $Y = F + E$, where $F \in \mathbb{R}^{N\times 1}$ contains the *noiseless* data $f(k)$, i.e. the noiseless version of $y(k)$, and $E \in \mathbb{R}^{N\times 1}$ contains the error terms $e(k)$. We will suppose now that the errors $e(k)$ are independent and normally distributed with variance σ^2. The distribution of the observed values given the noiseless ones is:

$$p\Big(Y \mid F\Big) = \mathcal{N}\Big(Y \mid F,\ \sigma^2 \cdot I_N\Big). \quad (4)$$

where $I_N \in \mathbb{R}^{N\times N}$ denotes the N-dimensional identity matrix. From the GP's definition the marginal distribution $p(F)$ is given by a Gaussian whose mean is zero and whose covariance is defined by the kernel matrix $\mathcal{K} \in \mathbb{R}^{N\times N}$:

$$p(F) = \mathcal{N}\Big(F \mid 0,\ \mathcal{K}\Big). \quad (5)$$

The matrix $\mathcal{K}$ (also known as Gram matrix) is a symmetric semidefinite positive matrix, such that $\mathcal{K}_{st} = k\big(s,t\big)$. Therefore, instead of placing a prior on the parameters, we put a prior over the noiseless data F. The marginal distribution of Y can be found by marginalizing over F, using known properties of Gaussian distributions (see Equation (2.115) of [2]), as:

$$\begin{aligned} p(Y) &= \int p(Y \mid F) \cdot p(F) dF \\ &= \mathcal{N}\Big(Y \mid 0,\ \mathcal{K} + \sigma^2 \cdot I_N\Big) \\ &= \mathcal{N}\Big(Y \mid 0,\ Z_\eta\Big). \end{aligned} \quad (6)$$

where $\eta = \left[\lambda, \beta, \sigma^2\right]^T \in \mathbb{R}^{3\times 1}$ contains the hyperparameters of the method. A prediction on a set of test data $Y_T \in \mathbb{R}^{N_T \times 1}$ can be obtained as the expected value of the predictive distribution $p\Big(Y_T \mid Y\Big)$. The predictive distribution can be computed by applying standard formulas for conditioned Gaussian distributions (see Equations $(2.81) - (2.82)$ of [2]). Its expected value is:

$$\widehat{Y}_T = \mathcal{K}_T \cdot Z_\eta^{-1} \cdot Y, \tag{7}$$

where $\mathcal{K}_T \in \mathbb{R}^{N_T \times N}$ is the kernel matrix such that its (s,t)-element is $k\big(s,t\big)$ with $t = 1, \ldots, N$, $s = 1, \ldots, N_T$.

The values of $\widehat{Y}_T = \left[\widehat{y}\left(1\right), \cdots, \widehat{y}\left(N_T\right)\right]^T \in \mathbb{R}^{N_T \times 1}$ are a noiseless estimate of the true function in correspondence of the test inputs. Therefore, they can be employed in place of the raw measurement data for further analysis. The method provides also the variance of the estimate $\Sigma_T \in \mathbb{R}^{N_T \times N_T}$ at the prediction points. In this work, we only perform smoothing: the test data are equal to the train data, such that $Y_T = Y$ and $N_T = N$.

For each impulse response, we performed an hyperparameters optimization procedure, by employing the Empirical Bayes method [2]. The technique consists into maximizing the *marginal likelihood* of the data (that depends on η) given by (6). An estimate of the hyperparameters values can be obtained as [2]:

$$\widehat{\eta} = \arg\min_{\eta} Y^T Z_\eta^{-1} Y + \log\det(Z_\eta). \tag{8}$$

To efficiently compute (8), we used the computational trick of Algorithm 2.1 in [13], that employs Cholesky decomposition of the marginal likelihood covariance matrix Z_η. The results of the applied procedere is shown in Figure 5, where it can be observed how the method has efficiently reduced the noise present in the data.

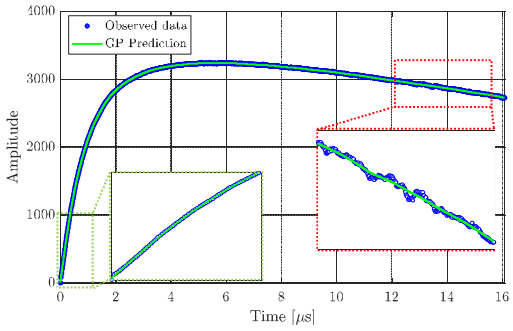

Fig. 5: Example of a measured impulse response (blue) with superimposed Gaussian Process prediction (green). The smothing effect is clearly visible

D. Subspace system identification

We now turn our attention to the identification of the system (1). Consider the state-space representation of discrete-time SISO LTI system:

$$x(k+1) = Ax(k) + Bu(k) \tag{9}$$

$$y(k) = Cx(k) + Du(k), \tag{10}$$

where $x(k) \in \mathbb{R}^{n\times 1}$, $u(k) \in \mathbb{R}$ and $y(k) \in \mathbb{R}$ are the system state (of dimension n), input and output, respectively. We set $D = 0$ since we preprocessed the impulse data to start from zero. With the data obtained by the flexible model devised in the previous section, a minimum-order realization of (9) can be found by employing the N4SID procedure described in [8], [12]. The method briefly consists into creating an Hankel matrix H composed by the noisy impulse measurements. The Singular Value Decomposition (SVD) is then employed to suitably reduce the rank of H to the chosen model order. With the reduced Hankel matrix, it is possible to obtain an estimate of the Observability and Reachability matrices of the system, from which an estimate $\left\{\widehat{A}, \widehat{B}, \widehat{C}\right\}$ can be computed.

Instead of creating the matrix H with the noisy data $\widetilde{v}(k)$, the idea is to use the smoothened ones $\widehat{y}(k)$, and apply the N4SID procedure. This approach permits to avoid optimization procedures that can get stuck in local minima, i.e. estimating the parameters of a predefined transfer function. As further check, the inspection of the SVD singular values showed that the order of the system is indeed three. After that the matrices $\left\{\widehat{A}, \widehat{B}, \widehat{C}\right\}$ are available, an estimate of the unkown parameters of (1), i.e. $\{\mu_f, \mu_s, \tau_f, \tau_s, \tau_m\}$ can be computed by converting the discrete system into a continous one. It should be noticed that this conversion can produce a couple of complex poles, that do not adhere with the modeling of (1). Those tests were discarded, resulting in the dataset of Table I. We leave to future research the case where N4SID results are used as initial condition for an optimization procedure.

The results of the N4SID procedure are perfectly in line with those obtained in [12]. Boxplots of the estimates are shown in Figures 6-9.

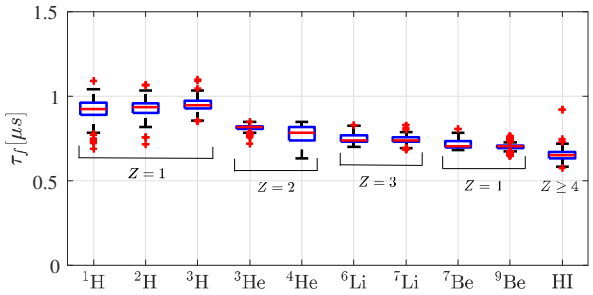

Fig. 6: Fast time constant

IV. Particles Classification

A particle type is completely defined by its *charge*, given by its atomic number Z, and its *mass*, given by its atomic mass number A. In the previous sections, we applied a system identification point of view to characterize each impulse response of light charged particles ($Z \leq 4$, $A \leq 9$). Following the separation principle, we first fit a low-bias model with gaussian process regression. Then, a model reduction has been performed. Each measurement is now condensed in an estimate of the parameters

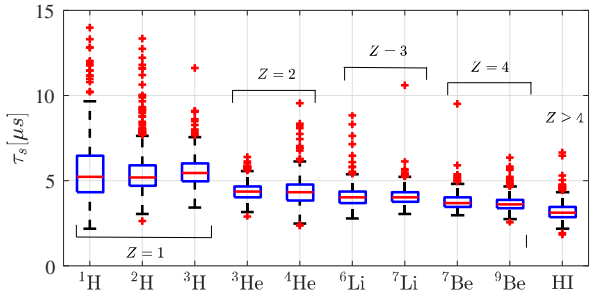

Fig. 7: Slow time constant

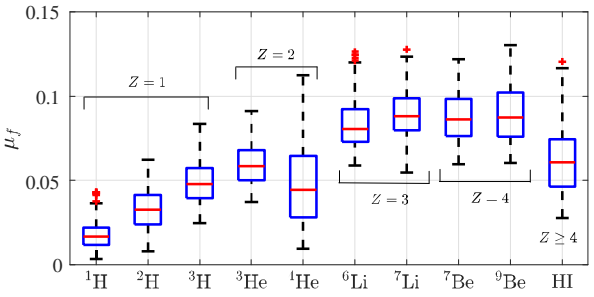

Fig. 8: Gain of the fast component

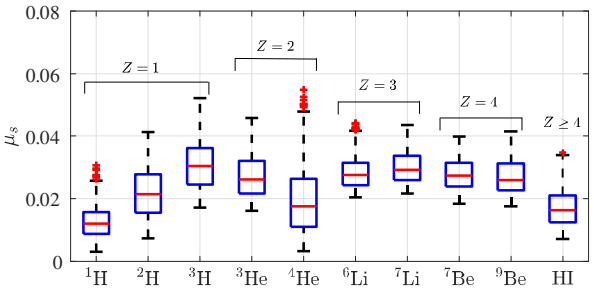

Fig. 9: Gain of the slow component

$\{\mu_f, \mu_s, \tau_f, \tau_s, \beta\}$. We can now represent each impulse response as a feature vector $\phi = [\mu_f, \mu_s, \tau_f, \tau_s, \beta]^T \in \mathbb{R}^{5\times 1}$. A feedforward neural network (NN) [2] is trained to predict, for each observation, its atomic number Z and atomic mass number A. The choice of using a NN model relies of the fact that it can efficiently handle multi-dimensional outputs as in this case. In fact, it is crucial to take into account label correlations during the classification process [4]. The NN is composed by 2 hidden layers with 10 neurons each, and a final layer with 2 outputs. The hidden layers have an hyperbolic tangent activation function. The NN structure has been chosen by cross validation. The output layer has a linear activation function. The labeled outputs consist in the couple $Q = [A, Z]^T \in \mathbb{R}^{2\times 1}$. The training data were standardized to zero mean on unitary variance. The same transformation, with mean and variance computed on the training set, is applied to the test data. The training of the NN has been performed using the well documented Levenberg-Marquardt minimization algorithm [6]. The NN predicts a vector $q = [q_1, q_2]^T \in \mathbb{R}^{2\times 1}$ which is the real-valued prediction of A and Z. The prediction were then rounded to the nearest integer value. The test set consisted in 100 samples from each type of particle. s The prediction of the NN model are then fed to a second classifier. A decision tree [3] is employed to predict the type of each particle. The inputs are the estimated values of A and Z, while the output is a integer number that represents the class of each observation. The complete classification procedure is reported in Figure 10. We could have employed just one classifier, mapping the features' vectors directly to the particle classes. However, the proposed chain of classifiers is not only taylored to the classification of different parciles, but it is also highly interpretable because they can be clustered according to the predicted atomic number Z and atomic mass number A, as will be show in the next section.

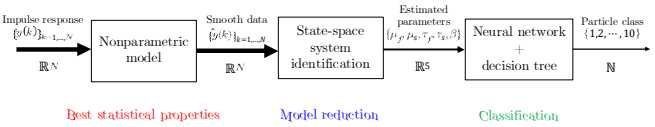

Fig. 10: Schematic of the classification procedure

V. Results and Discussion

Several observations can be made from the results of Figures 6-9. The mean value of fast time constant τ_f and of the slow one τ_s decreases (tendentially) with the atomic number Z. The standard deviation also decreases. The gains μ_f and μ_s tend to increase with Z and A, apart for the heavy ions (HI) and the ^{4}He particles. The hyperparameter β increses with Z. This is in line with the behaviour of τ_f and τ_s. Infact, lower time constants indicate a higher decay rate. This is the exact information that β encodes. These estimates are in line with the literature [12].

The classification results of the proposed approach are compared with the method proposed in [12]. Here, the author directly performed the N4SID step on noisy impulse data $\tilde{v}(k)$ (after data preprocessing). Notice how the task is quite challenging: infact, previous results obtained very high classification rates. In this work, we reimplemented the method proposed in [12] to make the comparison. The purpose is to test the effectiveness of the proposed two-step identification procedure. The classification accuracies are reported in Figure 11 and Figure 12. The heatmaps represent the percentage of corrected classifications, comparing the predicted particle types with the known ones. Darker colors indicate an higher classification accuracy. The proposed approach obtained a classification accuracy of 96%. The method in [12] correctly classified the 93% of the test particles. It is important to emphasize how a 3% improvement in classification accuracy is a significant contribution for this problem, since this is important to determine the properties of investigated physical phenomena. Figure 13 plots a subset of the test samples along with the classification bounds discovered by the decision tree. Notice how the learned bounds are very intuitive and could be set by human visual inspection.

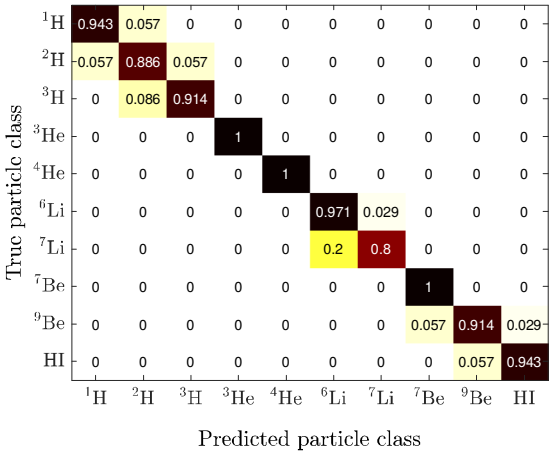

Fig. 11: Classification results of the method in [12]

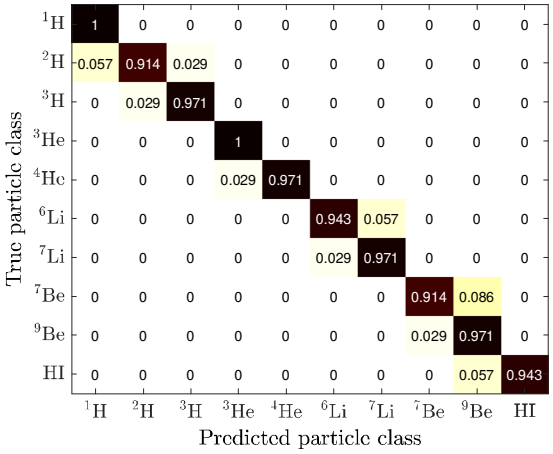

Fig. 12: Classification results of the proposed method

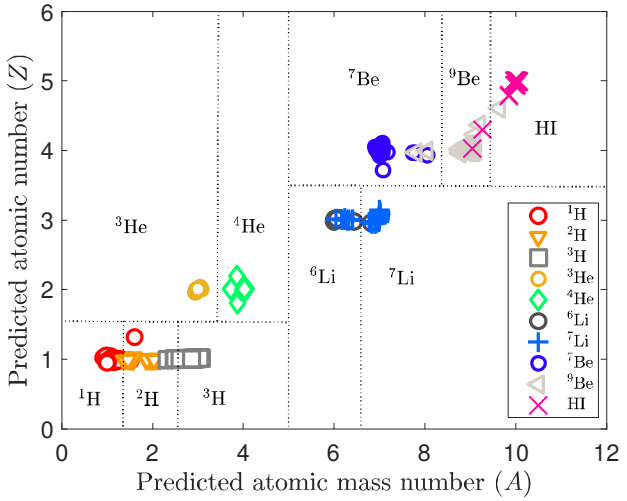

Fig. 13: A subset of test samples with the classification bounds learned by the decision tree

VI. Conclusions

In this paper, we investigated the use of the gaussian process framework to identify a low-bias dynamic model. The flexibility of GP permits to capture the dynamics that are required for a specific application. If a low-order model is needed, model reduction can be employed as subsequent step. This rationale has been applied to the classification of light charged particles. The parameters of the identified system are fed to a combination of classifiers to predict the particle type. The classification procedure is a black-box model that is, however, highly interpretable. Results showed how the combination of nonparametric and parametric modeling improved the classification accuracy of the previous method, that did not leveraged the nonparametric modeling step. Further research is devoted to a better investigation of the sensor's model, comparison with other model reduction techniques and the design of an ad-hoc kernel.

References

[1] S. Aiello, A. Anzalone, M. Baldo, G. Cardella, S. Cavallaro, E. De Filippo, A. Di Pietro, S. Femino, P. Figuera, P. Guazzoni, C. Iacono-Manno, G. Lanzan, U. Lombardo, S. Lo Nigro, A. Musumarra, A. Pagano, M. Papa, S. Pirrone, G. Politi, F. Porto, A. Rapisarda, F. Rizzo, S. Sambataro, M.L. Sperduto, C. Sutera, and L. Zetta. Chimera: a project of a 4π detector for heavy ion reactions studies at intermediate energy. *Nuclear Physics A*, 583:461–464, 1995.

[2] Christopher M. Bishop. *Pattern Recognition and Machine Learning (Information Science and Statistics)*. Springer-Verlag New York, Inc., Secaucus, NJ, USA, 2006.

[3] Jerome Friedman, Trevor Hastie, and Robert Tibshirani. *The elements of statistical learning*, volume 1. Springer series in statistics New York, 2001.

[4] Shantanu Godbole and Sunita Sarawagi. Discriminative methods for multi-labeled classification. In *Pacific-Asia conference on knowledge discovery and data mining*, pages 22–30. Springer, 2004.

[5] D.H.E. Gross. Statistical decay of very hot nuclei-the production of large clusters. *Reports on Progress in Physics*, 53(5):605, 1990.

[6] M. T. Hagan and M. B. Menhaj. Training feedforward networks with the marquardt algorithm. *IEEE Transactions on Neural Networks*, 5(6):989–993, Nov 1994.

[7] Hkan Hjalmarsson. From experiment design to closed-loop control. *Automatica*, 41(3):393 – 438, 2005. Data-Based Modelling and System Identification.

[8] A.M. King, U.B. Desai, and R.E. Skelton. A generalized approach to q-markov covariance equivalent realizations for discrete systems. *Automatica*, 24(4):507 – 515, 1988.

[9] Mirko Mazzoleni, Simone Formentin, Matteo Scandella, and Fabio Previdi. Semi-supervised learning of dynamical systems: a preliminary study. 2018. 17th IEEE European Control Conference (ECC), Lymassol, Cyprus.

[10] Mirko Mazzoleni, Matteo Scandella, Simone Formentin, and Fabio Previdi. Identification of nonlinear dynamical system with synthetic data: a preliminary investigation. 2018. 18th IFAC Symposium on System Identification (SYSID), Stockholm, Sweden.

[11] Gianluigi Pillonetto, Francesco Dinuzzo, Tianshi Chen, Giuseppe De Nicolao, and Lennart Ljung. Kernel methods in system identification, machine learning and function estimation: A survey. *Automatica*, 50(3):657 – 682, 2014.

[12] Fabio Previdi, Sergio M Savaresi, Paolo Guazzoni, and Luisa Zetta. Detection and clustering of light charged particles via system-identification techniques. *International Journal of Adaptive Control and Signal Processing*, 21(5):375–390, 2007.

[13] Carl Edward Rasmussen and Christopher K. I. Williams. *Gaussian Processes for Machine Learning (Adaptive Computation and Machine Learning)*. The MIT Press, 2005.

[14] W. Skulski and M. Momayezi. Particle identification in csi(tl) using digital pulse shape analysis. *Nuclear Instruments and Methods in Physics Research Section A: Accelerators, Spectrometers, Detectors and Associated Equipment*, 458(3):759 – 771, 2001.

[15] R. S. Storey, W. Jack, and A. Ward. The fluorescent decay of csi(tl) for particles of different ionization density. *Proceedings of the Physical Society,*, 72(1), 1958.